Received: 10 October 2020 | Revised: 12 November 2020 | Accepted: 3 December 2020

DOI: 10.1002/hbm.25319

RESEARCH ARTICLE

WILEY

Structural correlates underlying accelerated magnetic stimulation in Parkinson's disease

Gong-Jun Ji[1,2,3] | Tingting Liu[1,2,3] | Ying Li[1,2,3] | Pingping Liu[1,2,3] | Jinmei Sun[1,2,3] | Xingui Chen[1,2,3] | Yanghua Tian[1,2,3] | Xianwen Chen[1,2,3] | Louisa Dahmani[4] | Hesheng Liu[4] | Kai Wang[1,2,3] | Panpan Hu[1,2,3]

[1]Department of Neurology, The First Affiliated Hospital of Anhui Medical University, Hefei, China

[2]Collaborative Innovation Centre of Neuropsychiatric Disorder and Mental Health, Hefei, China

[3]Anhui Province Key Laboratory of Cognition and Neuropsychiatric Disorders, Hefei, China

[4]Department of Neuroscience, Medical University of South Carolina, Charleston, South Carolina

Correspondence
Kai Wang and Panpan Hu, Department of Neurology, The First Affiliated Hospital of Anhui Medical University, Hefei 230000, China.
Email: wangkai1964@126.com (K. W.) and hpppanda9@126.com (P. H.)

Hesheng Liu, Department of Neuroscience, Medical University of South Carolina, Charleston, SC.
Email: liuhe@musc.edu

Funding information
National Natural Science Foundation of China, Grant/Award Numbers: 81971689, 91432301, 31571149, 2016YFC1300604, 81790652; Collaborative Innovation Center of Neuropsychiatric Disorder and Mental Health of Anhui Province; Doctoral Foundation of Anhui Medical University, Grant/Award Number: XJ201532

Abstract

Repetitive transcranial magnetic stimulation (rTMS) is a noninvasive neuromodulation technique with great potential in the treatment of Parkinson's disease (PD). This study aimed to investigate the clinical efficacy of accelerated rTMS and to understand the underlying neural mechanism. In a double-blinded way, a total of 42 patients with PD were randomized to receive real (n = 22) or sham (n = 20) continuous theta-burst stimulation (cTBS) on the left supplementary motor area (SMA) for 14 consecutive days. Patients treated with real cTBS, but not with sham cTBS, showed a significant improvement in Part III of the Unified PD Rating Scale (p < .0001). This improvement was observed as early as 1 week after the start of cTBS treatment, and maintained 8 weeks after the end of the treatment. These findings indicated that the treatment response was swift with a long-lasting effect. Imaging analyses showed that volume of the left globus pallidus (GP) increased after cTBS treatment. Furthermore, the volume change of GP was mildly correlated with symptom improvement and associated with the baseline fractional anisotropy of SMA-GP tracts. Together, these findings implicated that the accelerated cTBS could effectively alleviate motor symptoms of PD, maybe by modulating the motor circuitry involving the SMA-GP pathway.

KEYWORDS
continuous theta-burst stimulation, functional connectivity, Parkinson's disease, transcranial magnetic stimulation

1 | INTRODUCTION

Parkinson's disease (PD) is a progressive neurodegenerative disorder affecting more than 6 million people worldwide (Schapira, 1999). Patients typically exhibit motor dysfunction including bradykinesia,

Gong-Jun Ji and Tingting Liu contributed equally to this work.

rigidity, resting tremor, and postural instability. The major pathological change is the loss of dopaminergic neurons in the substantia nigra (Burciu et al., 2017). Recent structural (Zeighami et al., 2015) and functional (Ji, Hu, et al., 2018) imaging studies suggested that PD is a network disorder involving both cortical and subcortical structures. Medical intervention can significantly improve PD symptoms, but severe complications such as dyskinesia and motor fluctuations can develop after long-term medication (Fahn, 2008). Less than 5% of PD patients can be further treated by deep brain stimulation (DBS) (Morgante et al., 2007), while for others, the treatment options are limited. It is thus important to develop alternative therapies for PD. Repetitive transcranial magnetic stimulation (rTMS) is a noninvasive brain stimulation technique that has been applied to PD patients in previous studies (Elahi & Chen, 2009; Pascual-Leone et al., 1994). While meta-analyses suggest that rTMS can alleviate motor symptoms in PD, conflicting results have emerged from randomized clinical trials (RCTs) (Chou, Hickey, Sundman, Song, & Chen, 2015; Chung & Mak, 2016; Wagle Shukla et al., 2016; Yang et al., 2018; Zanjani, Zakzanis, Daskalakis, & Chen, 2015). These inconsistent findings may be explained by the varied rTMS sequences and target selections used in these studies.

An optimal rTMS sequence is key to clinical efficacy. According to the meta-analysis, inhibitory rTMS on prefrontal cortex may alleviate symptoms of PD. 1-Hz rTMS and continuous theta-burst stimulation (cTBS) are two of the most frequently used protocols that can decrease the excitability of motor system (Huang, Edwards, Rounis, Bhatia, & Rothwell, 2005; Wischnewski & Schutter, 2015). However, cTBS is less time consuming. A typical cTBS session only takes 40 s, thus is extremely convenient for clinical application. Application of cTBS in patients also demonstrated potential for alleviation of motor symptoms in PD (Eggers, Gunther, Rothwell, Timmermann, & Ruge, 2015). Biochemical analysis (Volz, Benali, Mix, Neubacher, & Funke, 2013) and neuroimaging studies (Nettekoven et al., 2014) have demonstrated that three-block TBS (interval = 15 min) may produce cumulative effect. This multi-TBS protocol also showed significant efficacy in alleviating the symptoms of patients with schizophrenia (Chen et al., 2019). Thus, we hypothesized that this multi-TBS protocol will be effective in treating PD.

Another decisive factor of clinical efficacy is the TMS target. In PD, studies have tested the clinical efficiency of rTMS in several motor related areas, such as supplementary motor area (SMA), primary motor area, and dorsal prefrontal cortex (Chou et al., 2015). Among these clinical trials, Shirota et al. reported the highest symptom improvement after inhibitory rTMS on SMA (Shirota, Ohtsu, Hamada, Enomoto, & Ugawa, 2013). They defined the SMA as a 3-cm anterior leg motor area along the midline (Shirota et al., 2013). However, this landmark-based approach could be easily affected by the subjectivity of experimenters, making the results less reproducible. Given the anatomical variability of the human brain, image-navigation approach can improve the spatial precision of target and lead to better aftereffect of rTMS (Sack et al., 2009; Sparing, Buelte, Meister, Paus, & Fink, 2008). Although a protocol with multi-TBS and neuronavigated target may produce better clinical outcome, its efficacy in PD patients remains undetermined.

The neural mechanisms of TMS treatment for PD are only partially understood. TMS induces electrical current in the brain and modulates neural activity by changing local electrical environment (Di Lazzaro & Rothwell, 2014; Hamada, Murase, Hasan, Balaratnam, & Rothwell, 2013). However, imaging studies indicated that the stimulation not only changed the excitability of the target, but also affected regions distant to the target (Casula et al., 2017). A network theory has been proposed to explain this phenomenon (Fox et al., 2014). Although it is the superficial cortex that is directly modulated by TMS, the modulation effect could reach distant nodes of the target network. For instance, rTMS on dorsal prefrontal cortex induced structural changes in the rostral anterior cingulate cortex (rACC) in patients with depression, and the alteration was correlated with improvement in symptoms (Boes et al., 2018; Lan, Chhetry, Liston, Mann, & Dubin, 2016). The connectivity map of rACC has also been demonstrated as a valuable predictor for individual treatment effect (Fox et al., 2014; Weigand et al., 2017).

The network theory of rTMS also implicated the neural correlates in PD therapy (Fox et al., 2014). For example, SMA, an rTMS target for PD, is functionally connected to globus pallidus (GP), a DBS target. However, whether modulating SMA using TMS will lead to functional or anatomical changes in subcortical regions has not been examined in the context of a clinical trial for PD. Here, we carried out a double-blinded, randomized, sham-controlled study to examine the therapeutic efficacy of an optimized rTMS protocol. rTMS was optimized using three-block cTBS (Chen et al., 2019; Nettekoven et al., 2014) and MRI-guided target localization (Sack et al., 2009). We predicted that motor symptoms of PD patients would be alleviated through a consecutive 14-day treatment. We used structural and functional MRI to explore the neural correlates of motor symptom improvement after cTBS treatment.

2 | METHODS

2.1 | Standard protocol approvals, registrations, and patient consents

The study protocol was reviewed and approved by the institutional ethics committee of the First Affiliated Hospital of Anhui Medical University, and performed in accordance with the ethical standards as laid down in the 1964 Declaration of Helsinki and its later amendments. All participants provided written, informed consent before experiments. The study was registered at ClinicalTrials.gov with the identifier NCT02969941.

2.2 | Study design

According to a previous study (Brys et al., 2016), a parallel two-arm model (1:1; mean difference = 4.57 and *SD* = 4.9), yielded a sample size of 19 patients for each arm, providing 80% power with α level = .05. Participants were randomized into two groups by coin

tossing, and received real or sham rTMS over the left SMA on Day 1, followed by treatment for 14 consecutive days (Days 1–14). A researcher who was not involved in any aspect of the trial performed the randomization of participants. Multimodal MRI and symptom data were acquired for each participant on Days 1 and 15. To exclude the acute effect of medicine on symptom estimation and imaging features, all patients stopped consumption of medication for at least 12 hr (so-called "off" state) before these assessments. Patients and investigators were blind to group information. After the 14-day treatment (medication "on" state), the real treatment group was followed up for 2 months (4, 6, and 10 weeks after the first treatment).

2.3 | Participants

Participants were prospectively enrolled at the First Affiliated Hospital of Anhui Medical University from November 2016 through December 2018. The inclusion criteria were as follows: (a) diagnosis of idiopathic PD according to the UK Brain Bank Criteria, confirmed by a neurologist (author X. C.) with expertise in movement disorders; (b) ongoing treatment with a stable dose of any medication for 2 months; (c) 40 years of age or older; and (d) Mini-Mental State Examination (MMSE) score > 24. Exclusion criteria were as follows: (a) a history of addiction, psychiatric disorders, or neurological diseases other than PD; (b) focal brain lesions on T1-/T2-weighted fluid-attenuated inversion recovery images; (c) anti-PD medication adjustments during rTMS treatment; (d) history of substance abuse within the past 6 months; (e) nonremovable metal objects in or around the head; (f) previously received rTMS treatment; and (g) prior history of seizure or history in first-degree relatives.

2.4 | MRI-navigated rTMS

TMS was performed using a Magstim Rapid^2 transcranial magnetic stimulator (Magstim Company, Whitland, UK) with a 70-mm air-cooled figure-of-eight coil. All stimulations were guided by the participant's anatomical image ($1 \times 1 \times 1\ mm^3$) and a frameless neuronavigation system (Brainsight; Rogue Research, Montreal, QC, Canada). Each cTBS session lasted 40 s and consisted of three-pulse bursts at 50 Hz repeated every 200 ms (5 Hz) until a total of 600 pulses was reached (Huang et al., 2005). On each treatment day, patients received three rounds of cTBS separated by 15-min intervals (Chen et al., 2019; Ji, Yu, Liao, & Wang, 2017; Nettekoven et al., 2014; Volz et al., 2013). In total, 25,200 pulses were delivered during treatment (1,800 pulses per day). According to previous studies (Holtzheimer III et al., 2010), we termed this protocol that delivered high-dose stimulations in each treatment day as *accelerated cTBS*. The stimulation was delivered on the left SMA proper using Montreal Neurological Institute (MNI) coordinates (−6, −6, 77) (Ji et al., 2017) with intensity at 80% of the resting motor threshold (RMT). The coil was maintained horizontally pointing leftward, with its center positioned over the left SMA proper to maximize the strength of the electric field perpendicular to the target area. Patients in the sham rTMS group were treated using a placebo coil (Magstim Company) that produced a similar sound and sensation on scalp as the real coil but did not induce any current in the cortex. All the treatments were performed in the morning after usual drug intake. To ensure the double-blinded design, the rTMS operator (author T. L.) did not take part in any outcome assessment of the participants. At Week 2, patients were asked whether they were aware of their group assignment.

RMT was determined on the first day of the experiment by a five-step procedure (Schutter & van Honk, 2006). Briefly, the electromyography (EMG) signal of the abductor pollicis brevis muscle was recorded using Ag/AgCl surface electrodes, and displayed with the Rogue EMG device when the left "hand knob" area was activated by a single pulse stimulation. The RMT was defined as the lowest intensity evoking a small response (>50 μV) in more than 5 of 10 consecutive trials.

According to a previous RCT study, the left SMA is a potential effective target for PD (Shirota et al., 2013). The proper part of SMA is functionally connected to the GP (Ji et al., 2016), which is an effective DBS target for PD treatment (Fox et al., 2014). Accordingly to a recent network theory of neuromodulation targets (Fox et al., 2014), we restricted our target within the SMA proper, a sphere region centered in MNI coordinates (−6, −6, 77) with a 6-mm radius (Ji et al., 2017). The target was transformed into each participant's native space by applying an inverse matrix produced during brain structure segmentation using SPM12 (www.fil.ion.ucl.ac.uk/spm) and TMStarget (Ji et al., 2017) software.

2.5 | Symptom and neuropsychological assessments

Demographic information and neuropsychological scores were obtained before rTMS treatment. The neuropsychological tests included MMSE, Montreal Cognitive Assessment, Digit Span Test, Verbal Fluency Test, Hamilton Depression Rating Scale, and Hamilton Anxiety Rating Scale. Clinical symptoms were assessed with the Unified PD Rating Scale Part III (UPDRS-III, motor symptoms), Non-Motor Syndrome Scale (Chaudhuri et al., 2007), timed up-and-go test (Podsiadlo & Richardson, 1991), and 20-m walking test (Lomarev et al., 2006) at baseline and 1 and 2 weeks after the first treatment. Noted that patients were not required to walk as quickly as possible to complete the behavioral tests. The latter two tests were repeated three times and averaged at each time point. Dosages of anti-parkinsonian drugs are expressed as the levodopa equivalent dose using a recommended formula (Tomlinson et al., 2010).

The primary outcome of this study was improvement in UPDRS-III score at Week 2 (on Day 15 of the experiment) relative to baseline; responders were patients whose UPDRS-III score decreased by >30% from the baseline (Poewe et al., 2007).

2.6 | Multimodal MRI data acquisition and processing

Functional, structural, and diffusion MRI data were acquired with a 3-T scanner (Discovery 750; GE Healthcare, Milwaukee, WI) (Ji, Ren, et al., 2018).

2.6.1 | Structural data

High spatial resolution T1-weighted anatomic images were acquired in the sagittal orientation using a three-dimensional brain-volume sequence (repetition/echo time, 8.16/3.18 ms; flip angle, 12°; field of view, 256 × 256 mm^2; 256 × 256 matrix; section thickness, 1 mm, without intersection gap; voxel size, 1 × 1 × 1 mm^3; 188 sections).

Voxel-based morphometry (VBM) analysis was performed on the structural imaging data with the SPM12 toolbox Computational Anatomy Toolbox 12. For this longitudinal analysis, mean images of each patient were computed after inverse-consistent realignment and bias correction between different time points. The images were then segmented into gray matter (GM), white matter, and cerebrospinal fluid (Ashburner & Friston, 2005) and spatially normalized using the DARTEL algorithm (Ashburner, 2007). Normalization parameters were applied to the GM images at each time point. After visual inspections of preprocessed images, the modulated GM images were smoothed with a Gaussian kernel of 8 mm.

GM volume in motor network was analyzed using a two-way analysis of variance (ANOVA) with group as the between-subjects factor and time as the within-subject factor (at baseline and Week 2). Total intracranial volume was set as a nuisance variable to remove the related variance. The motor network was defined as in our previous work (Ji, Hu, et al., 2018; Ji, Ren, et al., 2018). It included bilateral primary motor/somatosensory cortices, paracentral lobules, SMA, thalamus, putamen, GP, and caudate nucleus from the automatic anatomical labeling template (Tzourio-Mazoyer et al., 2002). This image-based ANOVA was performed with SPM12 toolbox Statistic Non-parameter Mapping. According to Eklund, Nichols, and Knutsson (2016), we set a cluster-defined threshold $p < .01$, and reported the cluster-level corrected findings using permutation test (family-wise error controlled $p < .05$). Clusters with significant interaction effect were defined as the effective target ($target_{eff}$) of rTMS treatment.

2.6.2 | Diffusion MRI data

Diffusion data were acquired with a spin-echo echo planar imaging sequence, including 30 volumes with diffusion gradients applied along 30 noncollinear directions (b = 1,000 s/mm^2) and three volumes without diffusion weighting (b = 0 s/mm^2). Each volume consisted of 67 contiguous axial sections (TR = 8,600 ms, TE = 84.2 ms, flip angle = 90°, field of view = 256 × 256 mm^2, matrix = 128 × 128, slice thickness = 2 mm, no interslice gap).

Diffusion images were preprocessed and analyzed using the fMRIB Software Library (http://fsl.fmrib.ox.ac.uk/fsl). For each participant, head motion and eddy current-induced distortion were corrected with an eddy function. Fractional anisotropy (FA) maps were then generated by fitting the diffusion tensor model at each voxel. The probability distributions of fiber direction at each voxel were calculated using a probabilistic diffusion model (BED-POSTX function) in individual diffusion space.

The fiber bundles between SMA proper to $target_{eff}$ were identified by probabilistic tracking (Ji et al., 2016). Firstly, SMA and $target_{eff}$, as regions of interest (ROIs), were transformed into individual diffusion space in three steps: 1) the structural image was coregistered to a diffusion B0 image; 2) the structural image was normalized to the MNI space and the inverse matrix was obtained; and 3) the inverse matrix was applied to ROIs in the MNI space. Probabilistic tractography was applied by sampling 5,000 streamline fibers per voxel in the SMA ROI. Only samples that reached predefined ROIs were retained. FA values of tracks at a range of different thresholds (0.1, 0.2, and 0.3 of the maximal value in the tractography map) were averaged for statistical analysis.

2.6.3 | Functional MRI data

For resting-state fMRI scanning, participants were instructed to rest with their eyes closed without falling asleep. Functional images (217 volumes) were acquired using a single shot gradient-recalled echo planar imaging sequence (repetition/echo time, 2,400/30 ms; flip angle, 90°). Images of 46 transverse sections (field of view, 192 × 192 mm^2; 64 × 64 in-plane matrix; section thickness without intersection gap, 3 mm; voxel size, 3 × 3 × 3 mm^3) were acquired parallel to the anteroposterior commissure line.

Functional images were processed as in our previous studies (Chen et al., 2019; Ji et al., 2017) using DPARSF (Yan, Wang, Zuo, & Zang, 2016) (http://rfmri.org) and SPM12 toolkits. Briefly, the preprocessing included the following steps: (a) deletion of the first five volumes; (b) slice timing and realignment; (c) coregistration of structural to functional images; (d) normalization of functional images by DARTEL-based structural segmentation; (e) smoothing of functional images with a 4-mm isotropic Gaussian kernel; (f) temporal band-pass filtering (0.01–0.1 Hz); and (g) regressing out of 27 nuisance signals (three averages from white matter, cerebrospinal fluid, global brain, and 24 head motion parameters) (Friston, Williams, Howard, Frackowiak, & Turner, 1996).

2.7 | Statistical analysis

2.7.1 | Baseline and therapeutic efficacy

Baseline demographic and neuropsychological scores were compared between the two groups using independent two-sample t tests, except for male/female ratio which was assessed using a chi-squared test. Treatment outcomes (UPDRS-III, NMSS, timed up-and-go test, and 20-m walking test) were analyzed separately using two-way

ANOVAs with group (real and sham rTMS) as the between-subjects factor and time (baseline, Week 1, and Week 2) as the within-subjects factor. Post hoc analyses were performed using Sidak's multiple comparison test (Holm, 1979). Follow-up outcomes in the real group were compared to baseline using paired *t* tests. Response/nonresponder ratios were investigated at Week 1 and 2 using chi-squared tests. All analyses were performed with Prism v.6.0 (GraphPad Inc., La Jolla, CA).

2.7.2 | Imaging correlates of symptom improvement

Statistical analysis of GM volume is as described in Section 2.6.1, and significant clusters were defined as $target_{eff}$. Functional and structural connectivity between $target_{sti}$ and $target_{eff}$ were analyzed using two-way ANOVAs (group × time). Post hoc analyses were performed using Sidak's multiple comparison test (Holm, 1979). The association between significant MRI variables and change in UPDRS-III was assessed using Pearson's correlation if the data were normally distributed, otherwise Spearman's correlation was used.

3 | RESULTS

3.1 | Characteristics of the study population

Of the 64 patients who completed screening (Figure 1), 46 were randomized to receive cTBS, with 25 patients assigned to receive real stimulation to the SMA (Figure 2a) and 21 patients assigned to receive sham stimulation. Four patients withdrew before the primary endpoint (Week 2) due to personal reasons. Therefore, the primary outcome (UPDRS-III) was assessed in 22 patients in the real group and 20 patients in the sham group. Forty-one patients completed the other symptom and behavior tests. One patient in the sham group did not take part in the 20-m walking test at Weeks 1 and 2. Multimodal MRI data were acquired from 21 and 19 patients in the real and sham groups, respectively.

3.2 | Baseline measures

No significant difference was found between the real and sham groups in demographic (e.g., age), clinical (e.g., disease duration), or neuropsychological (e.g., MMSE) characteristics (Table 1).

3.3 | Primary outcome

Our primary outcome was the UPDRS-III score at Week 2 (Week 1 results are presented in the secondary outcomes section below). There was a significant interaction effect between time (baseline and Week 2) and group (real and sham) ($F_{1,40}$ = 30.34, p < .0001; Table 2 and Figure 2b). UPDRS-III scores (mean ± *SE*) showed a significant decrease in the real group (from 28.0 ± 2.12 at baseline to 20.6 ± 1.82 at Week 2; t = 7.0, p < .0001; 95% confidence interval [CI], 5.0–10.0) but not in the sham group (from 29.3 ± 2.03 to

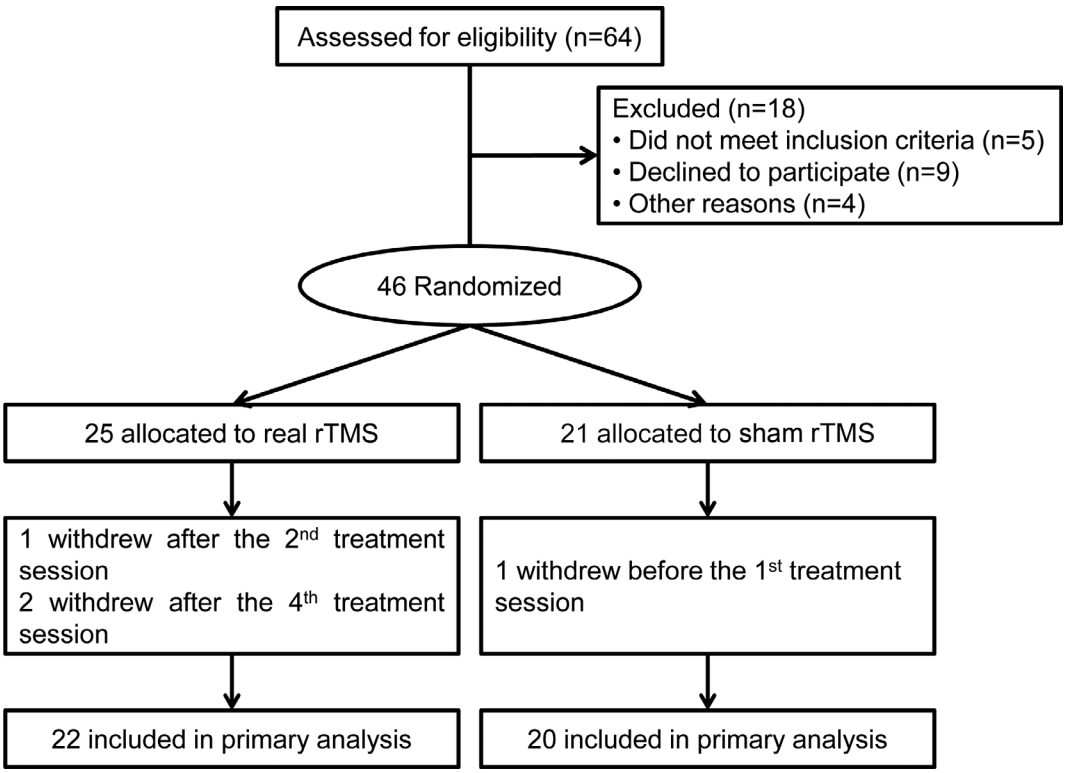

FIGURE 1 Schematic diagram elucidating randomization of patients with Parkinson's disease

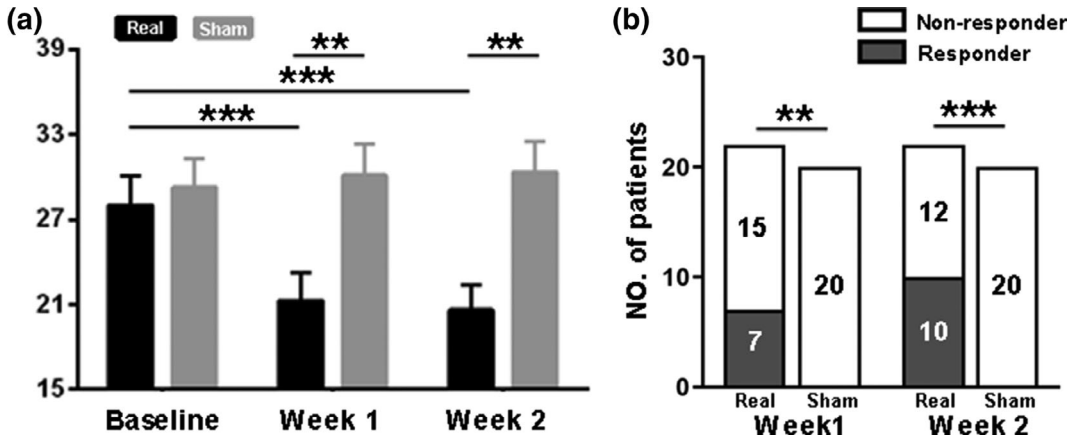

FIGURE 2 Outcome measures (mean ± *SE*) in real and sham treatment groups. After repetitive transcranial magnetic stimulation (rTMS)of the left supplementary motor area (SMA), a significant interaction effect was found for motor symptoms (a). Responders were participants with a UPDRS-III reduction >30%. The responder/nonresponders ratio is significantly higher in the real group than the sham group (b). NMSS, Non-Motor Symptom Scale; UPDRS-III, Unified Parkinson's Disease Rating Scale Part III. $^{*}p < .05$, $^{**}p < .01$, $^{***}p < .001$

TABLE 1 Baseline demographic and clinical measures

Measures	Real group	Sham group	Statistics	*p*
Sample size (m/f)	14/8	14/6	0.19[a]	.66
Age (years)	61.7 (1.57)	60.2 (1.97)	0.63[b]	.53
Education (years)	9.1 (1.13)	8.4 (0.98)	0.43[b]	.67
Duration (years)	4.3 (0.52)	5.3 (0.83)	1.00[b]	.33
UPDRS-III	28.0 (2.12)	29.3 (2.03)	0.44[b]	.66
NMSS	36.3 (4.35)	35.6 (3.89)	0.13[b]	.90
Timed up-and-go (s)	11.4 (0.48)	12.4 (1.04)	0.87[b]	.39
20 m walking (s)	23.8 (1.07)	23.3 (1.32)	0.29[b]	.77
H-Y	1.6 (0.12)	1.7 (0.11)	0.39[b]	.70
LED (mg)	485.2 (58.08)	460.5 (68.04)	0.27[b]	.79
MMSE	28.1 (0.42)	28.7 (0.41)	0.95[b]	.35
MoCA	24.2 (0.83)	24.6 (0.78)	0.32[b]	.75
VFT	17.9 (0.92)	17.6 (0.65)	0.27[b]	.79
DST (forward)	7.5 (0.28)	7.2 (0.28)	0.64[b]	.52
DST (backward)	4.1 (0.24)	3.6 (0.22)	1.66[b]	.11
HARS	8.7 (1.17)	8.1 (1.22)	0.39	.70
HDRS	8.1 (0.95)	7.8 (1.28)	0.19	.85

Note: Values in brackets indicate *SE*s.
Abbreviations: DST, digit span test; HARS, Hamilton Anxiety Rating Scale; HDRS, Hamilton Depression Rating Scale; LED, levodopa equivalent dose; MMSE, Mini-Mental State Examination; MoCA, Montreal cognitive assessment; NMSS, Non-Motor Syndrome Scale; UPDRS-III, Unified Parkinson's Disease Rating Scale Part III; VFT, verbal fluency test.
[a]Chi-squared test.
[b]Two-sample *t* test.

30.4 ± 2.16; $t = -0.95$, $p = .58$; 95% CI, −3.6 to 1.5). The scores at Week 2 were significantly lower in the real (20.6 ± 1.82) than sham (30.4 ± 2.16) group ($t = -3.39$, $p = .002$; 95% CI, −16.3 to 3.2).

3.4 | Secondary outcomes

Treatment-induced changes on the UPDRS-III from baseline to Week 1 showed a similar pattern as Week 2 ($F_{1,40} = 21.28$, $p < .0001$; Table 2 and Figure 2a). After 1-week cTBS, UPDRS-III scores decreased in the real (from 28.0 ± 2.12 to 21.3 ± 2.02; $t = 5.98$, $p < .0001$; 95% CI, 4.1–9.3) but not the sham group (from 29.3 ± 2.03 to 30.1 ± 2.22; $t = -0.68$, $p = .75$; 95% CI, −3.5 to 1.9). UPDRS-III scores were significantly lower in the real group than in the sham group at Week 1 ($t = -2.97$, $p = .008$; 95% CI, −15.6 to −2.1). The responder/nonresponder ratio was higher in the real group than in the sham group at both Week 1 ($\chi^2 = 8.32$, $p = .004$) and Week 2 ($\chi^2 = 12.9$, $p = .0003$) (Table 2 and Figure 2b). Specifically, treatment

TABLE 2 Symptom measures at Weeks 1 and 2

Measures	Real group	Sham group	Statistics	*p*
Primary outcome				
UPDRS-III (Week 2)	20.6 (1.82)	30.4 (2.16)	30.34[a]	<.0001
Secondary outcomes				
UPDRS-III (Week 1)	21.3 (2.02)	30.1 (2.22)	21.28[a]	<.0001
Responder/nonresponder ratio (Week 1)	7/15	0/20	8.32[b]	.004
Responder/nonresponder ratio (Week 2)	10/12	0/20	12.9[b]	.0003
NMSS (Week 1, 2)	22.9 (3.01), 21.9 (2.1)	25.1 (3.67), 26.8 (2.68)	0.72[a]	.49
Timed up-and-go (Week 1, 2)	10.9 (0.48), 10.7 (0.5)	11.9 (0.99)[c] 11.6 (1.21)[c]	0.42[a]	.66
20-m walking (Week 1, 2)	21.8 (1.03), 21.8 (1.05)	22.7 (1.48)[d], 22.9 (1.7)[d]	1.34[a]	.27

Note: Values in brackets indicate *SE*s.
Abbreviations: ANOVA, analysis of variance; NMSS, Non-Motor Syndrome Scale; UPDRS-III, Unified Parkinson's Disease Rating Scale Part III.
[a]Interaction effect in two-way ANOVA indicating outcome changes (from baseline to Week 1 and/or 2) between groups.
[b]Chi-squared test.
[c]Mean and *SE* were calculated based on 18 patients.
[d]Mean and *SE* were calculated based on 19 patients.

response (UPDRS-III score reduction >30%) was achieved in nearly half of the subjects (10 in 22) who received real treatment, whereas no response was achieved in the sham group. The baseline UPDRS-III was not significantly different between responders and nonresponders (t = 0.47, p = .65). When questioned at Week 2, the patients reported their group assignment at a chance level, indicating they were uncertain about the group assignment.

No significant interaction effects (two groups and three time points) were found for the NMSS, timed up-and-go, or 20-m walking test (Table 2), while a significant time effect was observed for the NMSS ($F_{2,80}$ = 16.6, p < .0001) and the 20-m walking test ($F_{2,78}$ = 3.92, p = .02).

3.5 | Adverse effects

The stimulation was well-tolerated. No adverse effect was reported in any group.

3.6 | Follow-up outcomes

After the 14-day treatment, UPDRS-III in the real group was evaluated at three follow-up time points, namely Week 4 (n = 16), Week 6 (n = 16), and Week 10 (n = 14). Sixteen patients participated in more than one follow-up. Twelve patients participated in all three follow-ups. We performed a mixed-measure ANOVA for these follow-ups and baselines. Significant treatment effect was found ($F_{1.5,21.4}$ = 28.93, p < .0001). Post hoc analysis (Bonferroni's correction) showed decreased UPDRS-III at Week 4 (t = 7.13, p < .0001; n = 15), Week 6 (t = 7.97, p < .0001; n = 15), and Week 10 (t = 5.58, p = .0003; n = 13), as compared to the baseline. These results suggest that the rTMS treatment has a long-lasting effect. More specifically, the reduction was maintained in 9 of the 10 responders at Week 10 (Figure 3a), and none of the nonresponders became responder in follow-ups (Figure 3b).

3.7 | Imaging correlates of symptom improvement

3.7.1 | Structural imaging

The VBM analysis showed a significant interaction effect in the left thalamus and GP (nonparametric test, family-wise error-corrected p < .05; Table S1; Figure 4a,b). The signal of the peak voxel in these two clusters was used for post hoc and correlation analyses. The normalized change in UPDRS-III (baseline minus Week 2, then divided by baseline) showed a mild correlation with volume increase in the left GP (ρ = .32, p = .04) (Figure 4c) but nonsignificant correlation with the left thalamus (r = .3, p = .06). Correlation between disease duration and volume change in the left GP (r = .10, p = .53) and thalamus (r = .19, p = .23) was not significant.

3.7.2 | Diffusion imaging

We then defined two ROIs in the left thalamus and GP. The thalamus ROI was defined as a sphere with a radius of 6 mm centered at the peak voxel. Considering the nonsphere contour of the GP cluster, the ROI was defined as the GP mask from the automated anatomical labeling template. Structural connectivity (i.e., FA) were estimated between stimulation target (i.e., SMA) and these two subcortical ROIs. Baseline FA values in SMA-GP tract showed a positive correlation with volume change of the GP (ρ = .56, p = .008, Figure 4d). FA values in SMA-thalamus tract was not correlated with volume change of the thalamus (r = .43, p = .054).

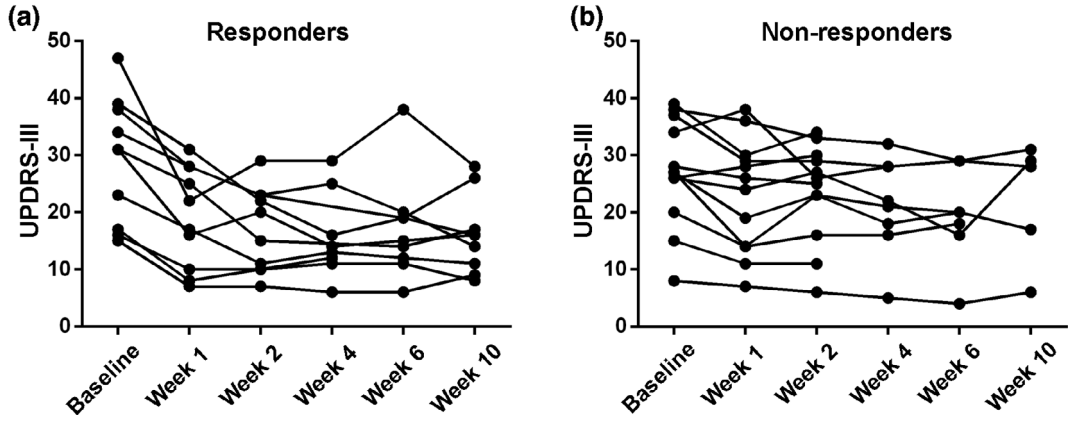

FIGURE 3 Individual changes on the Unified Parkinson's Disease Rating Scale Part III (UPDRS-III) in responders (a) and nonresponders (b) from the real stimulation group. Responders were patients whose UPDRS-III decreased by >30% from baseline

3.7.3 | Functional imaging

Resting-state functional connectivity between SMA and the two subcortical structures was not correlated with their volume changes (GP, ρ = –.27, p = .24; thalamus, r = .07, p = .78). Head motion, as measured by frame-wise displacement (Power, Barnes, Snyder, Schlaggar, & Petersen, 2012), showed no difference between groups at baseline (t = 0.82, p = .41).

4 | DISCUSSION

This RCT study investigated the efficacy of accelerated cTBS in the treatment of PD. The primary analysis showed that accelerated cTBS of the SMA significantly decreased UPDRS-III scores whereas sham stimulation did not. Treatment response (UPDRS-III score reduction >30%) was achieved in nearly half of the subjects (10 in 22) who received real treatment, whereas no response was achieved in the sham group. Furthermore, symptom improvement was observed as early as 1 week after treatment started. Follow-up examinations indicated that symptom improvement was maintained even 8 weeks after the end of treatment. Motor function improvement was mildly associated with structural changes in the left GP.

4.1 | Clinical efficacy of cTBS

This study indicated the efficacy of cTBS in treating PD symptoms. A significant decrease on the UPDRS-III (7.4 points on average) was observed after 2 weeks of real treatment, which represents a clinically significant improvement (Shulman et al., 2010), whereas no response was achieved in the sham treatment group. This cTBS-induced improvement appears to be higher than that induced by 1-Hz stimulation of the SMA (i.e., 6.84 points) (Shirota et al., 2013), although the difference should be directly compared in the same study in the future. Another RCT study also reported a significant clinical effect through 10-Hz stimulation of the primary motor area; however, the effect size of symptom improvement appeared to be lower (4.9 points) (Brys et al., 2016). These findings are consistent with those of previous meta-analyses (Chou et al., 2015; Yang et al., 2018) and provide evidence that inhibitory rTMS of the SMA can be an efficient therapy for PD.

Critically, the clinical effect in our study was observed after only 7 days of treatment, and maintained 8 weeks after the end of the treatment. This fast-acting and long-term maintenance may relate to the optimized settings of stimulation protocol. It has been shown that typical intermittent TBS (iTBS) and cTBS with 600 pulses (Huang et al., 2005) has similar modularity capacity on the MEP amplitude as conventional rTMS protocols, such as 1- or 5-Hz stimulations (Zafar, Paulus, & Sommer, 2008). An accelerated iTBS protocol, for example, repeating the iTBS for three times, could produce long aftereffect in both MEP and fMRI activity (Nettekoven et al., 2014). In schizophrenia, triple cTBS also produced a higher responder/nonresponder ratio than typical cTBS (Chen et al., 2019). Here, we found that the effect of this accelerated stimulation in PD may be stronger and longer than that shown in previous RCT reports (Brys et al., 2016; Shirota et al., 2013). Our findings also suggest that a long washout time (>2 months) should be used to exclude the residual effect in future studies with a crossover design.

4.2 | Structural correlates of rTMS treatment

The neural mechanism of rTMS treatment is still debated (Bergmann, Karabanov, Hartwigsen, Thielscher, & Siebner, 2016; Dayan, Censor, Buch, Sandrini, & Cohen, 2013; Fox et al., 2014; Hallett, 2007; Neggers, Petrov, Mandija, Sommer, & van den Berg, 2015). From a physiological point of view, the aftereffects of cTBS were usually explained by long-term depression, as the duration of the effects seem to suggest changes in synaptic plasticity. In PD, the impaired neuroplasticity has been shown in both animal model and human studies (Koch, 2013). For instance, no plasticity change was found in

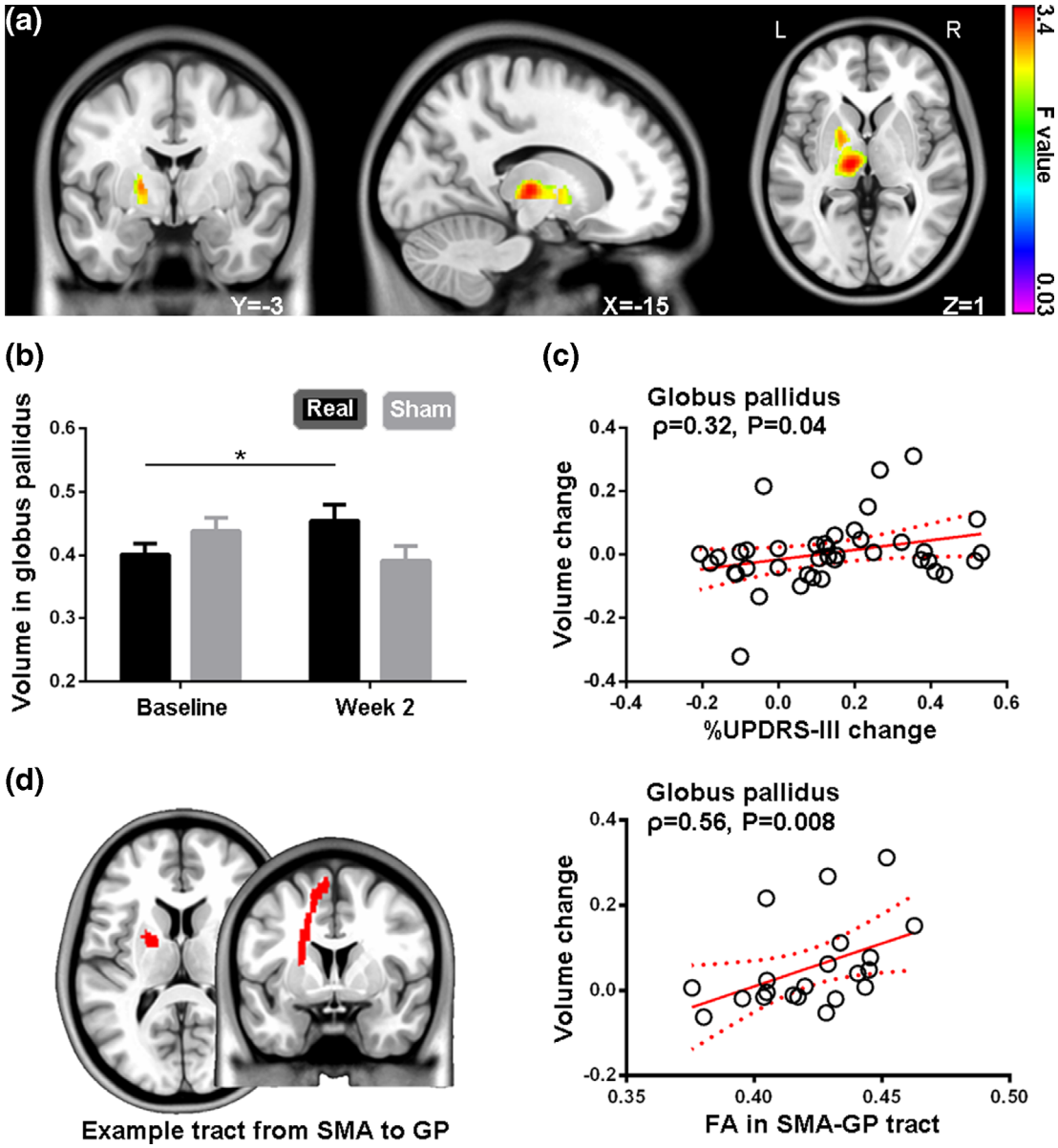

FIGURE 4 Neural correlates of the continuous theta-burst stimulation (cTBS) treatment effect. Voxel-based morphometric analysis showed a significant Interaction effect in the left thalamus and globus pallidus (GP) (a). Normalized symptom improvement was correlated with volume change in the GP (b). Fractional anisotropy of the tract from supplementary motor area to GP at baseline was positively correlated with the volume change in the GP (c)

de novo PD patients after rTMS stimulations (Kishore, Joseph, Velayudhan, Popa, & Meunier, 2012). It is possible that the efficiency of our treatment is partly contributed by restoring the cortical plasticity of patients. Future studies that estimate the change of neuroplasticity in motor system and associating it with symptom improvement are crucial to clarify this hypothesis.

In contrast to the cellular level mechanism, our MRI-based findings reflected the neural correlates in macrolevel. A significant volume increase was found in the left GP after real treatment. Similar structural changes after rTMS were also reported in both healthy participants (May et al., 2007) and patients (Boes et al., 2018; Hasan et al., 2017; Lan et al., 2016) previously. Furthermore, our data indicated that the structural pathway between SMA and GP may play a role in the modulation effect, as FA value of this pathway is related to the volume change of GP. The interna GP is an effective DBS target for PD (Follett et al., 2010) and has structural connectivity with the SMA. Our finding is in line with the network hypothesis (Fox et al., 2014) which suggested that effective rTMS and DBS therapies may work by modulating different nodes of the same functional network. Additionally, our findings implicate a predictive value of baseline structural connectivity for clinical outcome. To achieve better symptom improvement, future studies may need to define personalized SMA target in subregion showing the highest structural connectivity with GP. In contrast to the structural findings, the functional

connectivity between SMA and GP did not show significant relation with symptom or volume changes. This negative result may be probably due to the instability of resting-state fMRI in estimating single link (Pannunzi et al., 2017), when the scanning duration is not long enough (e.g., ~8 min). According to reliability studies (Birn et al., 2013; Noble et al., 2017), multisessions (>30 min) should be performed for future studies. Taken together, our data suggest that the modulation effect of SMA stimulation in PD is likely dependent on the SMA-GP pathway (Andoh, Matsushita, & Zatorre, 2015; Voineskos et al., 2010).

4.3 | Limitations

Several limitations in this study are worth mentioning. First, this is a single-center study and the findings must be confirmed in a large-scale clinical trial. Second, all patients received medical intervention during the rTMS treatment. To exclude the acute effect of medication on the findings, symptom and imaging data were acquired for patients in medication "off" state. However, the long-term effect of medicine still persisted. To completely rule out the contribution of medication (e.g., its interaction with rTMS) on the clinical improvement in the real group, future studies with drug-naïve patients are still necessary. Third, in this study, participants were allocated using coin flipping. Although this simple randomization can achieve random assignment, it cannot prevent the imbalances in the sample size. This method is more suitable for large-scale clinical trials. For small sample studies, adaptive randomization may be a better choice (Lim & In, 2019). Fourth, although TMS coil was placed on the center of SMA, the stimulation may also significantly modulate the function of the neighboring gyrus (Deng, Lisanby, & Peterchev, 2013). Thus, it should be noted that the clinical outcome and treatment mechanism may be partly contributed from gyrus adjacent to the left SMA. By estimating the induced electric field individually, future studies may clarify to what extent cortices outside the left SMA was effectively modulated in rTMS treatment (Weise, Numssen, Thielscher, Hartwigsen, & Knosche, 2020). Fifth, the RMT was not tested every day before the treatment. Although our previous study did not find significant difference between RMTs estimated within subjects 1 week apart (Ji et al., 2017), future work considering the intraindividual variability (Sommer, Wu, Tergau, & Paulus, 2002) may further improve the treatment efficiency. Finally, additional attention should be paid to the RMT testing in PD patients. In definition, the RMT should be tested on the patient in a relaxed state. However, rigid PD patients may need longer time to relax their skeletal muscles than controls. In this study, the EMG signal was monitored by the navigation system in real time, and no prominent EMG signal (> 10 μv) was found before RMT testing. However, to further exclude the potential bias, a statistical comparison should be performed between groups for the EMG signal before RMT testing.

5 | CONCLUSION

This RCT suggests that the accelerated cTBS of left SMA is an effective treatment for alleviating PD motor symptoms. This particular stimulation protocol is fast acting and has a long-lasting effect. Structural pathway between SMA and GP may play an important role in this treatment.

ACKNOWLEDGMENTS

The authors thank the participants for taking part in the study. This study was funded by the National Key R&D Program of China (No. 2018YFC1314200 to P.H.); the National Natural Science Foundation of China (Nos. 81971689 to G.-J. J., 31970979, 91432301, 31571149, and 2016YFC1300604 to K. W. ; No. 81971072 to X.C.; No. 81790652 to H. L.; No. 81803130 to X.C.; No. 32071054 to Y.T.); Doctoral Foundation of Anhui Medical University (No. XJ201532 to G.- J. J.); and Collaborative Innovation Center of Neuropsychiatric Disorder and Mental Health of Anhui Province.

CONFLICT OF INTEREST

The authors declare no conflict of interest.

DATA AVAILABILITY STATEMENT

The data that support the findings of this study are available on request from the corresponding author.

ORCID

Gong-Jun Ji https://orcid.org/0000-0002-7073-5534
Jinmei Sun https://orcid.org/0000-0002-9295-2759
Yanghua Tian https://orcid.org/0000-0001-5038-0599
Kai Wang https://orcid.org/0000-0002-6197-914X

REFERENCES

Andoh, J., Matsushita, R., & Zatorre, R. J. (2015). Asymmetric interhemispheric transfer in the auditory network: Evidence from TMS, resting-state fMRI, and diffusion imaging. *The Journal of Neuroscience*, *35*, 14602–14611.

Ashburner, J. (2007). A fast diffeomorphic image registration algorithm. *NeuroImage*, *38*, 95–113.

Ashburner, J., & Friston, K. J. (2005). Unified segmentation. *NeuroImage*, *26*, 839–851.

Bergmann, T. O., Karabanov, A., Hartwigsen, G., Thielscher, A., & Siebner, H. R. (2016). Combining non-invasive transcranial brain stimulation with neuroimaging and electrophysiology: Current approaches and future perspectives. *NeuroImage*, *140*, 4–19.

Birn, R. M., Molloy, E. K., Patriat, R., Parker, T., Meier, T. B., Kirk, G. R., … Prabhakaran, V. (2013). The effect of scan length on the reliability of resting-state fMRI connectivity estimates. *NeuroImage*, *83*, 550–558.

Boes, A. D., Uitermarkt, B. D., Albazron, F. M., Lan, M. J., Liston, C., Pascual-Leone, A., … Fox, M. D. (2018). Rostral anterior cingulate cortex is a structural correlate of repetitive TMS treatment response in depression. *Brain Stimulation*, *11*, 575–581.

Brys, M., Fox, M. D., Agarwal, S., Biagioni, M., Dacpano, G., Kumar, P., … Pascual-Leone, A. (2016). Multifocal repetitive TMS for motor and mood symptoms of Parkinson disease: A randomized trial. *Neurology*, *87*, 1907–1915.

Burciu, R. G., Ofori, E., Archer, D. B., Wu, S. S., Pasternak, O., McFarland, N. R., … Vaillancourt, D. E. (2017). Progression marker of Parkinson's disease: A 4-year multi-site imaging study. *Brain: A Journal of Neurology*, *140*, 2183–2192.

Casula, E. P., Stampanoni Bassi, M., Pellicciari, M. C., Ponzo, V., Veniero, D., Peppe, A., … Koch, G. (2017). Subthalamic stimulation and

levodopa modulate cortical reactivity in Parkinson's patients. *Parkinsonism & Related Disorders*, *34*, 31–37.

Chaudhuri, K. R., Martinez-Martin, P., Brown, R. G., Sethi, K., Stocchi, F., Odin, P., … Schapira, A. H. (2007). The metric properties of a novel non-motor symptoms scale for Parkinson's disease: Results from an international pilot study. *Movement Disorders*, *22*, 1901–1911.

Chen, X., Ji, G. J., Zhu, C., Bai, X., Wang, L., He, K., … Wang, K. (2019). Neural correlates of auditory verbal hallucinations in schizophrenia and the therapeutic response to theta-burst transcranial magnetic stimulation. *Schizophrenia Bulletin*, *45*(2), 474–483.

Chou, Y. H., Hickey, P. T., Sundman, M., Song, A. W., & Chen, N. K. (2015). Effects of repetitive transcranial magnetic stimulation on motor symptoms in Parkinson disease: A systematic review and meta-analysis. *JAMA Neurology*, *72*, 432–440.

Chung, C. L., & Mak, M. K. (2016). Effect of repetitive transcranial magnetic stimulation on physical function and motor signs in Parkinson's disease: A systematic review and meta-analysis. *Brain Stimulation*, *9*, 475–487.

Dayan, E., Censor, N., Buch, E. R., Sandrini, M., & Cohen, L. G. (2013). Noninvasive brain stimulation: From physiology to network dynamics and back. *Nature Neuroscience*, *16*, 838–844.

Deng, Z. D., Lisanby, S. H., & Peterchev, A. V. (2013). Electric field depth-focality tradeoff in transcranial magnetic stimulation: Simulation comparison of 50 coil designs. *Brain Stimulation*, *6*, 1–13.

Di Lazzaro, V., & Rothwell, J. C. (2014). Corticospinal activity evoked and modulated by non-invasive stimulation of the intact human motor cortex. *The Journal of Physiology*, *592*, 4115–4128.

Eggers, C., Gunther, M., Rothwell, J., Timmermann, L., & Ruge, D. (2015). Theta burst stimulation over the supplementary motor area in Parkinson's disease. *Journal of Neurology*, *262*, 357–364.

Eklund, A., Nichols, T. E., & Knutsson, H. (2016). Cluster failure: Why fMRI inferences for spatial extent have inflated false-positive rates. *Proceedings of the National Academy of Sciences of the United States of America*, *113*, 7900–7905.

Elahi, B., & Chen, R. (2009). Effect of transcranial magnetic stimulation on Parkinson motor function—Systematic review of controlled clinical trials. *Movement Disorders*, *24*, 357–363.

Fahn, S. (2008). The history of dopamine and levodopa in the treatment of Parkinson's disease. *Movement Disorders*, *23*(Suppl 3), S497–S508.

Follett, K. A., Weaver, F. M., Stern, M., Hur, K., Harris, C. L., Luo, P., … Reda, D. J. (2010). Pallidal versus subthalamic deep-brain stimulation for Parkinson's disease. *The New England Journal of Medicine*, *362*, 2077–2091.

Fox, M. D., Buckner, R. L., Liu, H., Chakravarty, M. M., Lozano, A. M., & Pascual-Leone, A. (2014). Resting-state networks link invasive and noninvasive brain stimulation across diverse psychiatric and neurological diseases. *Proceedings of the National Academy of Sciences of the United States of America*, *111*, E4367–E4375.

Friston, K. J., Williams, S., Howard, R., Frackowiak, R. S., & Turner, R. (1996). Movement-related effects in fMRI time-series. *Magnetic Resonance in Medicine*, *35*, 346–355.

Hallett, M. (2007). Transcranial magnetic stimulation: a primer. *Neuron*, *55*, 187–199.

Hamada, M., Murase, N., Hasan, A., Balaratnam, M., & Rothwell, J. C. (2013). The role of interneuron networks in driving human motor cortical plasticity. *Cerebral Cortex*, *23*, 1593–1605.

Hasan, A., Wobrock, T., Guse, B., Langguth, B., Landgrebe, M., Eichhammer, P., … Koutsouleris, N. (2017). Structural brain changes are associated with response of negative symptoms to prefrontal repetitive transcranial magnetic stimulation in patients with schizophrenia. *Molecular Psychiatry*, *22*, 857–864.

Holm, S. (1979). A simple sequentially rejective multiple test procedure. *Scandinavian Journal of Statistics*, *6*, 65–70.

Holtzheimer, P. E., III, McDonald, W. M., Mufti, M., Kelley, M. E., Quinn, S., Corso, G., & Epstein, C. M. (2010). Accelerated repetitive transcranial magnetic stimulation for treatment-resistant depression. *Depression and Anxiety*, *27*, 960–963.

Huang, Y. Z., Edwards, M. J., Rounis, E., Bhatia, K. P., & Rothwell, J. C. (2005). Theta burst stimulation of the human motor cortex. *Neuron*, *45*, 201–206.

Ji, G. J., Hu, P., Liu, T. T., Li, Y., Chen, X., Zhu, C., … Wang, K. (2018). Functional connectivity of the corticobasal ganglia-thalamocortical network in Parkinson disease: A systematic review and meta-analysis with cross-validation. *Radiology*, *287*(3), 973–982.

Ji, G. J., Liao, W., Yu, Y., Miao, H. H., Feng, Y. X., Wang, K., … Zang, Y. F. (2016). Globus pallidus interna in Tourette syndrome: Decreased local activity and disrupted functional connectivity. *Frontiers in Neuroanatomy*, *10*, 93.

Ji, G. J., Ren, C., Li, Y., Sun, J., Liu, T., Gao, Y., … Wang, K. (2018). Regional and network properties of white matter function in Parkinson's disease. *Human Brain Mapping*, *40*(4), 1253–1263.

Ji, G. J., Yu, F., Liao, W., & Wang, K. (2017). Dynamic aftereffects in supplementary motor network following inhibitory transcranial magnetic stimulation protocols. *NeuroImage*, *149*, 285–294.

Kishore, A., Joseph, T., Velayudhan, B., Popa, T., & Meunier, S. (2012). Early, severe and bilateral loss of LTP and LTD-like plasticity in motor cortex (M1) in de novo Parkinson's disease. *Clinical Neurophysiology*, *123*, 822–828.

Koch, G. (2013). Do studies on cortical plasticity provide a rationale for using non-invasive brain stimulation as a treatment for Parkinson's disease patients? *Frontiers in Neurology*, *4*, 180.

Lan, M. J., Chhetry, B. T., Liston, C., Mann, J. J., & Dubin, M. (2016). Transcranial magnetic stimulation of left dorsolateral prefrontal cortex induces brain morphological changes in regions associated with a treatment resistant major depressive episode: An exploratory analysis. *Brain Stimulation*, *9*, 577–583.

Lim, C. Y., & In, J. (2019). Randomization in clinical studies. *Korean Journal of Anesthesiology*, *72*, 221–232.

Lomarev, M. P., Kanchana, S., Bara-Jimenez, W., Iyer, M., Wassermann, E. M., & Hallett, M. (2006). Placebo-controlled study of rTMS for the treatment of Parkinson's disease. *Movement Disorders*, *21*, 325–331.

May, A., Hajak, G., Ganssbauer, S., Steffens, T., Langguth, B., Kleinjung, T., & Eichhammer, P. (2007). Structural brain alterations following 5 days of intervention: Dynamic aspects of neuroplasticity. *Cerebral Cortex*, *17*, 205–210.

Morgante, L., Morgante, F., Moro, E., Epifanio, A., Girlanda, P., Ragonese, P., … Savettieri, G. (2007). How many parkinsonian patients are suitable candidates for deep brain stimulation of subthalamic nucleus? Results of a questionnaire. *Parkinsonism & Related Disorders*, *13*, 528–531.

Neggers, S. F., Petrov, P. I., Mandija, S., Sommer, I. E., & van den Berg, N. A. (2015). Understanding the biophysical effects of transcranial magnetic stimulation on brain tissue: The bridge between brain stimulation and cognition. *Progress in Brain Research*, *222*, 229–259.

Nettekoven, C., Volz, L. J., Kutscha, M., Pool, E. M., Rehme, A. K., Eickhoff, S. B., … Grefkes, C. (2014). Dose-dependent effects of theta burst rTMS on cortical excitability and resting-state connectivity of the human motor system. *The Journal of Neuroscience*, *34*, 6849–6859.

Noble, S., Spann, M. N., Tokoglu, F., Shen, X., Constable, R. T., & Scheinost, D. (2017). Influences on the test-retest reliability of functional connectivity MRI and its relationship with behavioral utility. *Cerebral Cortex*, *27*, 5415–5429.

Pannunzi, M., Hindriks, R., Bettinardi, R. G., Wenger, E., Lisofsky, N., Martensson, J., … Deco, G. (2017). Resting-state fMRI correlations: From link-wise unreliability to whole brain stability. *NeuroImage*, *157*, 250–262.

Pascual-Leone, A., Valls-Sole, J., Brasil-Neto, J. P., Cammarota, A., Grafman, J., & Hallett, M. (1994). Akinesia in Parkinson's disease. II. Effects of subthreshold repetitive transcranial motor cortex stimulation. *Neurology*, *44*, 892–898.

Podsiadlo, D., & Richardson, S. (1991). The timed "up & go": A test of basic functional mobility for frail elderly persons. *Journal of the American Geriatrics Society*, *39*, 142–148.

Poewe, W. H., Rascol, O., Quinn, N., Tolosa, E., Oertel, W. H., Martignoni, E., … Boroojerdi, B. (2007). Efficacy of pramipexole and transdermal rotigotine in advanced Parkinson's disease: A double-blind, double-dummy, randomised controlled trial. *The Lancet Neurology*, *6*, 513–520.

Power, J. D., Barnes, K. A., Snyder, A. Z., Schlaggar, B. L., & Petersen, S. E. (2012). Spurious but systematic correlations in functional connectivity MRI networks arise from subject motion. *NeuroImage*, *59*, 2142–2154.

Sack, A. T., Cohen Kadosh, R., Schuhmann, T., Moerel, M., Walsh, V., & Goebel, R. (2009). Optimizing functional accuracy of TMS in cognitive studies: A comparison of methods. *Journal of Cognitive Neuroscience*, *21*, 207–221.

Schapira, A. H. (1999). Science, medicine, and the future: Parkinson's disease. *BMJ*, *318*, 311–314.

Schutter, D. J., & van Honk, J. (2006). A standardized motor threshold estimation procedure for transcranial magnetic stimulation research. *The Journal of ECT*, *22*, 176–178.

Shirota, Y., Ohtsu, H., Hamada, M., Enomoto, H., & Ugawa, Y. (2013). Supplementary motor area stimulation for Parkinson disease: A randomized controlled study. *Neurology*, *80*, 1400–1405.

Shulman, L. M., Gruber-Baldini, A. L., Anderson, K. E., Fishman, P. S., Reich, S. G., & Weiner, W. J. (2010). The clinically important difference on the unified Parkinson's disease rating scale. *Archives of Neurology*, *67*, 64–70.

Sommer, M., Wu, T., Tergau, F., & Paulus, W. (2002). Intra- and interindividual variability of motor responses to repetitive transcranial magnetic stimulation. *Clinical Neurophysiology*, *113*, 265–269.

Sparing, R., Buelte, D., Meister, I. G., Paus, T., & Fink, G. R. (2008). Transcranial magnetic stimulation and the challenge of coil placement: A comparison of conventional and stereotaxic neuronavigational strategies. *Human Brain Mapping*, *29*, 82–96.

Tomlinson, C. L., Stowe, R., Patel, S., Rick, C., Gray, R., & Clarke, C. E. (2010). Systematic review of levodopa dose equivalency reporting in Parkinson's disease. *Movement Disorders*, *25*, 2649–2653.

Tzourio-Mazoyer, N., Landeau, B., Papathanassiou, D., Crivello, F., Etard, O., Delcroix, N., … Joliot, M. (2002). Automated anatomical labeling of activations in SPM using a macroscopic anatomical parcellation of the MNI MRI single-subject brain. *NeuroImage*, *15*, 273–289.

Voineskos, A. N., Farzan, F., Barr, M. S., Lobaugh, N. J., Mulsant, B. H., Chen, R., … Daskalakis, Z. J. (2010). The role of the corpus callosum in transcranial magnetic stimulation induced interhemispheric signal propagation. *Biological Psychiatry*, *68*, 825–831.

Volz, L. J., Benali, A., Mix, A., Neubacher, U., & Funke, K. (2013). Dose-dependence of changes in cortical protein expression induced with repeated transcranial magnetic theta-burst stimulation in the rat. *Brain Stimulation*, *6*, 598–606.

Wagle Shukla, A., Shuster, J. J., Chung, J. W., Vaillancourt, D. E., Patten, C., Ostrem, J., & Okun, M. S. (2016). Repetitive transcranial magnetic stimulation (rTMS) therapy in Parkinson disease: A meta-analysis. *PM & R: The Journal of Injury, Function, and Rehabilitation*, *8*, 356–366.

Weigand, A., Horn, A., Caballero, R., Cooke, D., Stern, A. P., Taylor, S. F., … Fox, M. D. (2017). Prospective validation that subgenual connectivity predicts antidepressant efficacy of transcranial magnetic stimulation sites. *Biological Psychiatry*, *84*(1), 28–33.

Weise, K., Numssen, O., Thielscher, A., Hartwigsen, G., & Knosche, T. R. (2020). A novel approach to localize cortical TMS effects. *NeuroImage*, *209*, 116486.

Wischnewski, M., & Schutter, D. J. (2015). Efficacy and time course of theta burst stimulation in healthy humans. *Brain Stimulation*, *8*, 685–692.

Yan, C. G., Wang, X. D., Zuo, X. N., & Zang, Y. F. (2016). DPABI: Data processing and analysis for (resting-state) brain imaging. *Neuroinformatics*, *14*, 339–351.

Yang, C., Guo, Z., Peng, H., Xing, G., Chen, H., McClure, M. A., … Mu, Q. (2018). Repetitive transcranial magnetic stimulation therapy for motor recovery in Parkinson's disease: A meta-analysis. *Brain and Behavior*, *8*, e01132.

Zafar, N., Paulus, W., & Sommer, M. (2008). Comparative assessment of best conventional with best theta burst repetitive transcranial magnetic stimulation protocols on human motor cortex excitability. *Clinical Neurophysiology*, *119*, 1393–1399.

Zanjani, A., Zakzanis, K. K., Daskalakis, Z. J., & Chen, R. (2015). Repetitive transcranial magnetic stimulation of the primary motor cortex in the treatment of motor signs in Parkinson's disease: A quantitative review of the literature. *Movement Disorders*, *30*, 750–758.

Zeighami, Y., Ulla, M., Iturria-Medina, Y., Dadar, M., Zhang, Y., Larcher, K. M., … Dagher, A. (2015). Network structure of brain atrophy in de novo Parkinson's disease. *eLife*, *4*.

SUPPORTING INFORMATION

Additional supporting information may be found online in the Supporting Information section at the end of this article.

How to cite this article: Ji G-J, Liu T, Li Y, et al. Structural correlates underlying accelerated magnetic stimulation in Parkinson's disease. *Hum Brain Mapp*. 2021;42:1670–1681. https://doi.org/10.1002/hbm.25319